Resistivity and magnetoresistance of amorphous Fe_xGe_{1-x} alloys near the metal-insulator transition

1993 J. Phys.: Condens. Matter 5 6067

(http://iopscience.iop.org/0953-8984/5/33/016)

J. Phys.: Condens. Matter 5 (1993) 6067–6082. Printed in the UK

Resistivity and magnetoresistance of amorphous Fe_xGe_{1-x} alloys near the metal–insulator transition

A Albers and D S McLachlan

Department of Physics and Condensed Matter Physics Research Unit, University of the Witwatersrand, Private Bag 3, WITS, 2050 Republic of South Africa

Received 14 October 1992, in final form 13 May 1993

Abstract. Electrical transport mechanisms near the metal–insulator transition are investigated in the amorphous Fe_xGe_{1-x} system ($0.05 \leqslant x \leqslant 0.30$) by measuring the resistivity between 100 mK and 273 K and the magnetoresistance between 100 mK and 6 K in magnetic fields up to 3.86 T. In the metallic samples, an anomalous dip in the resistivity is observed on cooling below 50 K, followed by an increase in the resistivity below about 10 K. The results of the measurements are compared to the predictions of current theories of variable-range hopping with interactions on the insulating side of the transition, and electron–electron interactions and weak localization on the metallic side of the transition.

1. Introduction

Over the last few decades a great deal of experimental and theoretical work has been carried out in order to try to understand the electrical transport mechanisms near the metal–insulator transition in disordered systems. In spite of all this effort, a clear picture has still not emerged. It is therefore of interest to make further resistivity and magnetoresistance measurements in selected systems, in order to provide a larger base of data that can be used to develop a physical understanding of the transport mechanisms involved. The aim of the present study is to investigate these mechanisms by extending the previous studies in the amorphous Fe_xGe_{1-x} alloy system to lower temperatures and to include magnetoresistance measurements near the metal–insulator transition for the first time.

Previously Daver *et al* (1974) and Massenet *et al* (1974) measured the resistivity of a-Fe_xGe_{1-x} thin films in the temperature range 20 K to 300 K for $0 \leqslant x \leqslant 0.64$. They observed $\rho = \rho_0 \exp(T_0/T)^{1/4}$ variable-range hopping conduction in all samples with $x \leqslant 0.25$. For larger x they concluded that conduction was metallic. Similar results for the a-Fe_xGe_{1-x} system have been obtained by Nath *et al* (1975), Chopra and Nath (1976), and Watanabe *et al* (1979). Cros (1980, 1981) measured the resistivity and magnetoresistance of samples with $x \geqslant 0.30$, which are well into the metallic regime. A need therefore exists for extended measurements of the resistivity and magnetoresistance of samples ranging from a few atomic percent to 30 at.% Fe, with an emphasis on samples near the metal–insulator transition.

2. Experimental method

a-Fe_xGe_{1-x} films, with a thickness of about 500 Å, have been prepared using Ar ion-beam sputtering. Prior to sputtering, separate Au voltage and very large current contacts were

0953-8984/93/336067+16$07.50

evaporated onto flame polished glass substrates, to facilitate good electrical contact as well as good thermal contact through the current leads for measurements below 1 K. The base pressure in the sputtering plant was 2×10^{-5} Pa, with a pressure of about 8×10^{-4} Pa maintained during the sputtering. The sputtering rate was typically about 5 Å min^{-1}. The thickness of the films was determined to ±10 Å using an oscillating quartz crystal thickness monitor, and checked using a Talystep stylus. During the deposition, the substrates were rotated at 6 rpm and held at −78 °C to ensure that homogeneous and amorphous films were produced. The amorphous nature of the films was confirmed by studying the films prepared under these conditions but deposited onto very thin amorphous silicon nitride windows, using electron diffraction on a transmission electron microscope. The diffraction patterns observed showed the broad diffuse rings characteristic of amorphous material. Using the half width of the observed rings, the maximum scale of crystalline order was estimated to be 10 Å. A sample geometry of 4 mm between voltage contacts by 3 mm wide was chosen to give a homogeneity in the resistivity (checked in a separate experiment using a four-point probe method) of better than 1%, which is equivalent to 0.67% in composition.

Films of different compositions were produced by changing the amount of pure Ge in a composite $Ge/Fe_{30}Ge_{70}$ target. The composition of the films was determined using EDAX (energy dispersive analysis of x-rays) compared to bulk Fe, Ge, and $Fe_{0.3}Ge_{0.7}$ standards, to ±0.3 at.% Fe. The thickness and composition of the films are given in table 1. Subsequent to preparation, the films were allowed to age at room temperature for a period of at least 20 d, during which period the resistivity increased by about 10% to a relatively stable value.

Table 1. The thickness, composition, and characteristic resistivities of the samples. The samples have been divided into two groups—metallic and insulating.

Name	Sample	Thickness (Å)	at.% Fe	$\rho(10)(\mu\Omega$ cm)	$\rho(0)(\mu\Omega$ cm)
A2.1	1	580(10)	28.0(3)	1729.4(2)	2000
A2.3	2	510(10)	23.2(3)	2352.4(2)	2700
A2.4	3	500(10)	20.5(3)	2933.9(2)	3300
A2.11	4	580(10)	20.1(3)	5030.4(2)	—
A2.19	5	610(10)	19.5(3)	9089.7(2)	32000
A2.17	6	570(10)	18.5(3)	10109(2)	21000
A2.22	7	660(10)	16.5(3)	17139(2)	110000
A2.10	8	520(10)	15.7(3)	$54.868(2) \times 10^3$	∞
A2.20	9	560(10)	15.0(3)	$104.89(2) \times 10^3$	∞
A2.7	10	520(10)	11.0(3)	$4315(1) \times 10^4$	∞
A2.8	11	520(10)	8.3(3)	$8359(1) \times 10^6$	∞
A2.5	12	510(10)	6.1(3)	$4480(1) \times 10^8$	∞

Four-point resistivity and magnetoresistance measurements were performed in three sets of experimental apparatus. Initial measurements of the resistance between 273 K and 4.5 K were made using a quick-measurement probe which was cooled by slowly inserting it into a liquid He storage dewar. In a conventional ^{4}He cryostat the resistance between 273 K and 1.2 K, and the magnetoresistance, at fixed temperatures between 4 K and 1.2 K (±0.2 K for $T \geqslant 30$ K, and ±0.01 K for 30 K > $T \geqslant$ 1.2 K), in varying fields ($\boldsymbol{B} \perp \boldsymbol{I}$ and $\boldsymbol{B} \perp$ plane of sample) up to 3.86 T have been measured. In this system the magnetoresistance was measured as a function of field at fixed temperatures. In both of the above two experiments, the measurements were made using a DC measurement system with a current density of 6 A cm^{-2} for the metallic samples, and between 6 A cm^{-2} and 60 μA cm^{-2} for the insulating

samples. The accuracy of the system was 1 in 10^5 using a $6\frac{1}{2}$-digit DVM for the metallic samples, and 1 in 10^4 using a Keithley electrometer for the insulating samples. For these measurements, leads were attached to the Au contact pads on the sample using Ag paint. Using a dilution refrigerator, the resistance and magnetoresistance at temperatures varying between 6 K and typically 100 mK (to ±1%) was measured in fixed fields from 0 to 4 T ($\boldsymbol{B} \perp \boldsymbol{I}$ or $\boldsymbol{B} \| \boldsymbol{I}$) using a Linear Research LR-400 AC resistance bridge to an accuracy of 1 in 10^5 with a current density of 60 mA cm^{-2}. Current contacts to the samples were made in this case by clamping the flattened ends of two Au wires onto the previously mentioned Au pads which covered the outer third of the substrates, thereby ensuring good thermal contact to the sample. The voltage leads were attached with Ag paint as before.

3. Experimental results

Table 1 shows the numbering, composition, thickness, and some characteristic resistivities for the samples. The observed resistivity as a function of temperature for the various samples is shown in figure 1. It will be shown that below 16 at.% Fe the samples show insulating-type behaviour, with $\rho \to \infty$ as $T \to 0$, while samples with more than 16 at.% Fe exhibit metallic-type behaviour (i.e. ρ remains finite as $T \to 0$). Above 50 K the resistivity of the latter samples shows typical negative temperature coefficient of resistance behaviour of high-resistivity metallic samples (Mooij 1973), levelling off below 50 K, but in some instances (samples 2, 3, and 4) displays a very unusual slight decrease at 50 K, which is illustrated in figure 2. The only other instances of similar behaviour are in the results of Möbius *et al* (1985) for a-Cr_xSi_{1-x} and the recent results for a-Cr_xGe_{1-x} of Elefant *et al* (1991). For all metallic samples at some point below 10 K, the resistivity shows a sharp increase with decreasing T, which eventually becomes proportional to $\sqrt{T}$. Figure 3(*a*) and (*b*) shows plots of σ against $\sqrt{T}$ for samples 3 and 5 with 20.5 and 19.5 at.% Fe respectively in different magnetic fields up to 3.86 T.

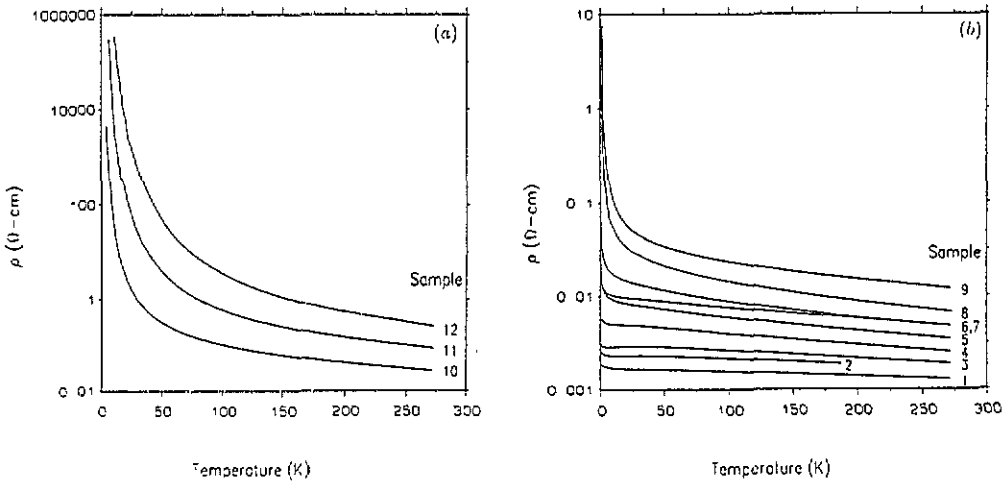

Figure 1. Log resistivity plotted against temperature for the a-Fe_xGe_{1-x} alloys: (*a*) samples 10, 11, and 12; (*b*) samples 1–9. The numbers on the plots are the sample numbers given in table 1. The composition of each sample is given in table 1.

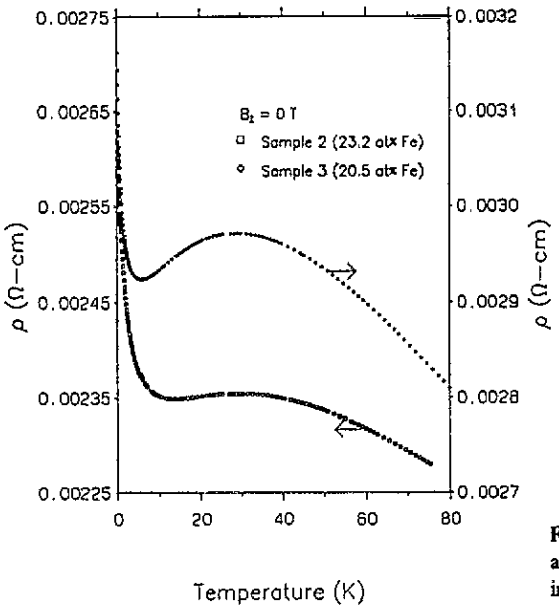

Figure 2. Plot of ρ against T showing the anomalous behaviour in the 10–50 K temperature interval.

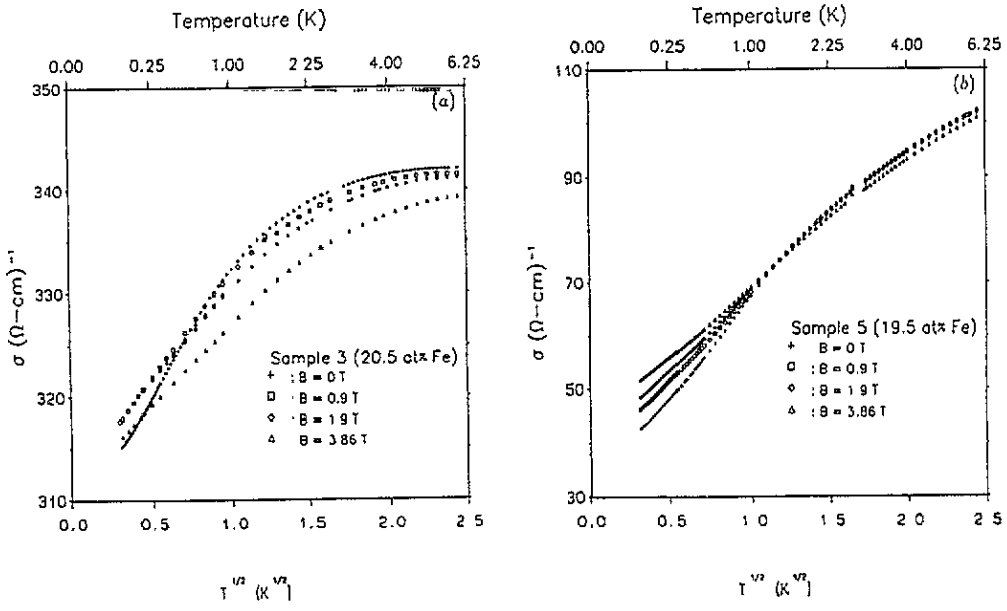

Figure 3. Plot of σ against $\sqrt{T}$, in various magnetic fields, illustrating the clear $\sqrt{T}$ dependence observed at low enough temperatures in (a) for sample 3 (20.5 at.% Fe) and in (b) for sample 5 (19.5 at.% Fe). The slight levelling off in ρ below 130 mK appears to be due to the loss of thermal contact between the samples and the tail of the dilution refrigerator.

The magnetoresistance behaviour, illustrated in figure 4(a)–(c) for samples 1, 6, and 9 respectively, falls into three main groups. As shown in figure 4(a), the most metallic sample (sample 1: 28 at.% Fe) has a negative magnetoresistance for all temperatures below 4 K, the magnitude of which increases as T decreases. Samples with between 24 at.% and 16 at.%

Fe (samples 2–7) show positive magnetoresistance at the higher temperatures, changing over to negative magnetoresistance at lower temperatures, the distinction between positive and negative magnetoresistance being based on the slope of the magnetoresistance at zero field. The temperature at which the cross-over from positive to negative magnetoresistance occurs is non-monotonic and depends on both the sample and the field. For instance, it goes from 1.4 K for 24 at.% to 0.2 K for 20.5 at.% and 1.2 K for 16 at.% in 3.86 T. Typical magnetoresistance curves for this class of sample are shown in figure 4(*b*) (sample 6: 18.5 at.% Fe). For an insulating sample close to the transition the magnetoresistance is very small and positive at very low fields in the region of 4 K, but becomes negative and very large with increasing B and decreasing T. This behaviour is shown in figure 4(*c*) (sample 9: 15.0 at.% Fe). The magnetoresistance of samples that were more insulating was also negative and appeared to become as large as 50% in 3.86 T, but because of the concurrent large variations in the resistance due to unavoidable small drifts in temperature, no accurate results could be obtained.

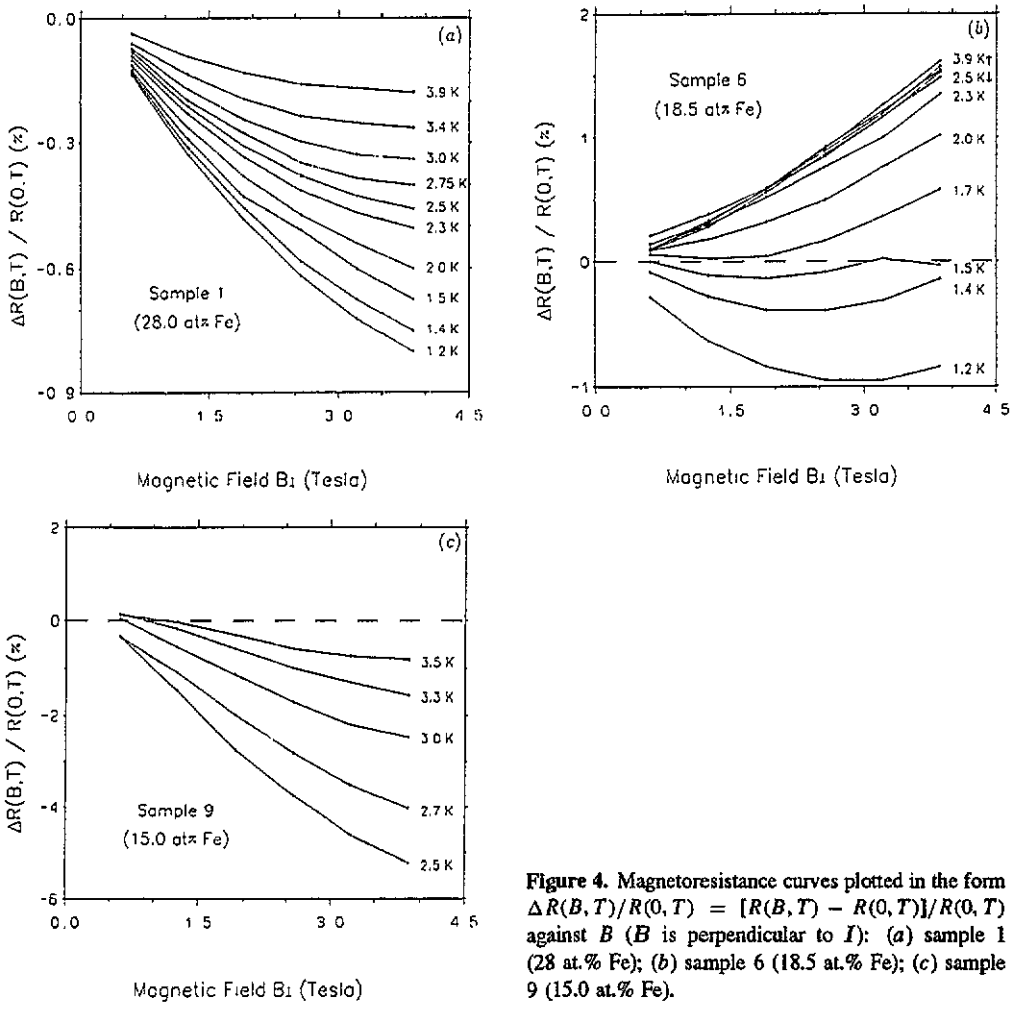

Figure 4. Magnetoresistance curves plotted in the form $\Delta R(B,T)/R(0,T) = [R(B,T) - R(0,T)]/R(0,T)$ against B (B is perpendicular to I): (*a*) sample 1 (28 at.% Fe); (*b*) sample 6 (18.5 at.% Fe); (*c*) sample 9 (15.0 at.% Fe).

4. Discussion

4.1. Insulating samples (< 16 at.% Fe)

A number of workers have investigated the resistivity of a-Ge and its alloys in the insulating regime. They have, in general, observed variable-range hopping conduction behaviour of the form

$$\rho = \rho_0 \exp(T_0/T)^n \tag{1}$$

with $n = (p+1)/(d+p+1)$ (Adkins 1989). Here, d is the dimensionality of the sample and p is the index of the energy dependence of the density of states at the Fermi level. Note that $n = \frac{1}{4}(\frac{1}{3})$ for 3D (2D) hopping for an energy-independent density of states, i.e. $p = 0$ (Mott 1968), and $n = \frac{1}{2}$ if Coulomb interaction effects are included, as $p = 2$ for $d = 3$, and $p = 1$ for $d = 2$ (Efros and Shklovskii 1975).

The dominance of $\exp(T_0/T)^{1/4}$ variable-range hopping has been reported for both pure a-Ge (Knotek *et al* 1973, Pollak *et al* 1973) and for a-Fe_xGe_{1-x} films up to 25 at.% Fe (Daver *et al* 1974, Massenet *et al* 1974, Nath *et al* 1975, Chopra and Nath 1976, Watanabe *et al* 1979). Both $\exp(T_0/T)^{1/2}$ and $\exp(T_0/T)^{1/4}$ variable-range hopping have also been reported for a number of other amorphous and crystalline systems (see the review by Shklovskii and Efros (1984)).

In the present experiments it was found to be rather difficult to distinguish between $\exp(T_0/T)^{1/2}$ and $\exp(T_0/T)^{1/4}$ behaviour by plotting $\ln \rho$ against $T^{-1/2}$ or $T^{-1/4}$, or even by fitting the data using the non-linear minimization routine MINUIT (James and Roos 1975). In order to overcome this problem, following White and McLachlan (1986), the data for the insulating samples have been plotted in figure 5 in the form $\mathrm{d}\ln g/\mathrm{d}\ln T$ against $\ln g$, where g is the conductance $(1/R)$ expressed in units of $e^2/\pi h = 7.7 \times 10^{-5}\Omega^{-1}$. The data for this graph were determined from the numerical derivative of a set of shape-preserving cubic splines that were fitted to the original numerical resistivity data. The inherent noise and digitial nature of the data explains the scatter of the points in some regions. It can easily be shown that data which follow $\rho \propto \exp(T_0/T)^n$, if plotted in this form, will appear as a straight line of slope $-n$. In figure 5, the data clearly show better agreement with a slope of $-\frac{1}{2}$. Therefore it is believed that the present insulating samples all show $\rho \propto \exp(T_0/T)^{1/2}$ behaviour at low temperatures.

Using the results from figure 5 as a criterion, the resistivity of the insulating samples has been fitted using MINUIT to expression (1) in the temperature range where $n \simeq \frac{1}{2}$. The fitting parameters were ρ_0, T_0 and n. The values of these parameters for the samples with $\lesssim 15.7$ at.% Fe (samples 9–12) are given in table 2, together with the temperature ranges over which the fits were made. The data between 10 K and 20 K ($\ln g < -10$) for sample 12 (6.1 at.% Fe) (which could only be measured down to 10 K) have been excluded from the fit because the noise on these very-high-resistance data is relatively large compared to the noise on the lower-resistance data at higher temperatures. Sample 8 (15.7 at.% Fe) also showed evidence of $\rho \propto \exp(T_0/T)^{1/2}$ behaviour, but only at temperatures below about 2 K. Because of this limited temperature range over which the data could be fitted, it is uncertain whether this is truly an insulating sample. As it is very close to the transition it could be heterogeneous, containing both insulating and metallic regions.

Following the formulation of Adkins (1989), an estimate of the tunnelling exponent α ($\alpha = a_0^{-1}$, where a_0 is the localization radius) can be made using the values of T_0 obtained from the range over which the data fitted (1), and the expression (in 3D)

$$\alpha = k_B T_0 (\pi g_2)^{1/3}/10.5 \tag{2}$$

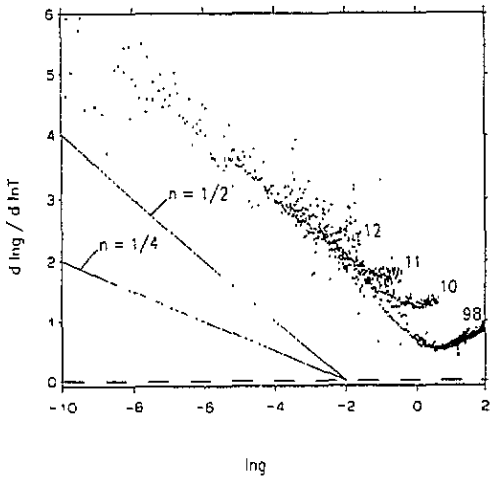

Figure 5. Plot of d ln g/d ln T against ln g, where g is the conductance $(1/R)$ in units of $e^2/\pi\hbar = 7.7 \times 10^{-5}\Omega^{-1}$, for the insulating samples (samples 8–12, < 16 at.% Fe). The sample numbers on the graph correspond to those given in table 1. The full lines indicate the expected behaviour for data that shows $\rho \propto \exp(T_0/T)^n$ for $n = \frac{1}{2}$ and $n = \frac{1}{4}$.

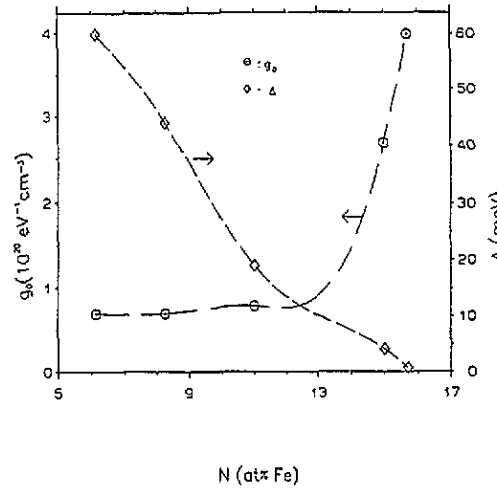

Figure 6. The values of the unperturbed density of states g_0 and the energy gap Δ, calculated from the fit parameters and equations (4) and (5), as a function of the concentration of Fe on the insulating side of the transition. The curves are drawn to guide the eye.

Table 2. Values of the hopping conduction parameters determined by fitting the ρ versus T data to the expression $\rho = \rho_0 \exp(T_0/T)^n$. The fits were made over the indicated temperature ranges.

Sample	ρ_0 (Ω cm)	T_0(K)	n	T range (K)
8 (15.7 at.% Fe)	0.0055(1)	35(1)	0.52(1)	1.1–2.22
9 (15.0 at.% Fe)	0.013(2)	42(2)	0.51(2)	1.2–58
10 (11.0 at.% Fe)	0.0070(8)	670(10)	0.49(2)	4.5–121
11 (8.3 at.% Fe)	0.0061(6)	1900(20)	0.50(2)	4.5–138
12 (6.1 at.% Fe)	0.0079(7)	3500(30)	0.49(2)	20–150

where $g_2 = [3^8\pi^2\epsilon_0^3/2^5e^6]\epsilon_r^3$, e is the electronic charge, ϵ_0 is the vacuum permittivity constant, ϵ_r is the actual dielectric constant of the material, and k_B is the Boltzmann constant. According to scaling theory, near the metal–insulator transition, the dielectric constant scales for $N < N_c$ as (Rosenbaum *et al* 1983)

$$\epsilon(N) = \epsilon_r = \epsilon(0)(1 - N/N_c)^{-\zeta} \tag{3}$$

where N_c is the critical doping concentration at the metal–insulator transition, and ζ is the critical exponent. Measurements on the metal–insulator transition in other systems (Rosenbaum *et al* 1983) indicate $\zeta \simeq 1$. Assuming that the dopant concentration N scales linearly as the concentration of Fe in the materials in the limited range of 5–15 at.% Fe, and using $N_c \simeq 16$ at.% Fe and $\epsilon(0) = 16$ (Phillips 1968), the dielectric constant for the different samples may be estimated (table 3), and hence the value of α may be calculated using (2). Typical values of α range from 9×10^7 m^{-1} to 7.6×10^8 m^{-1}, corresponding to values of a_0 of 110 Å (15.0 at.% Fe) to 13 Å (6.1 at.% Fe). Using the radial distribution

function results of Uemura *et al* (1977), the mean Fe–Fe distance is estimated to lie between 5 Å and 8 Å for $Fe_{0.1}Ge_{0.9}$. The values of α calculated above indicate that on the insulating side of the transition the mobile electrons are localized over about two Fe–Fe distances in the most insulating sample (sample 12: 6.1 at.% Fe), increasing to about 17 Fe–Fe distances near the metal–insulator transition. If $\epsilon(0) = 16$ is used for ϵ_r instead of the divergent form given by (3), the value of a_0 ranges from 21 Å to 2200 Å, which is not as physically realistic.

Table 3. Values of the actual dielectric constant ϵ_r (calculated using (3)), the tunnelling exponent α, the unperturbed density of states g_0, the energy gap Δ (in eV), and T_Δ (in K) where $T_\Delta = \Delta/k_B$. α, g_0, and Δ were calculated from the parameters of table 2 as explained in the text.

Sample	ϵ_r	α (10^8 m^{-1})	g_0 (eV^{-1} cm^{-3})	Δ (eV)	T_Δ (K)
8 (15.7 at.% Fe)	852(2)	2.5(1)	$4(1) \times 10^{20}$	$7.6(2) \times 10^{-4}$	8.8(2)
9 (15.0 at.% Fe)	256(1)	0.90(5)	$2.7(4) \times 10^{20}$	$4.1(2) \times 10^{-3}$	47(2)
10 (11.0 at.% Fe)	51.2(2)	2.87(5)	$7.89(7) \times 10^{19}$	$1.90(6) \times 10^{-2}$	220(6)
11 (8.3 at.% Fe)	33.1(2)	5.3(1)	$6.98(6) \times 10^{19}$	$4.4(1) \times 10^{-2}$	510(12)
12 (6.1 at.% Fe)	25.9(1)	7.6(1)	$6.98(6) \times 10^{19}$	$6.0(1) \times 10^{-2}$	690(13)

If the upper temperature limit for fitting the data to $\rho = \rho_0 \exp(T_0/T)^n$ in table 2 is considered to be the parameter T_c (the temperature below which the effect of the Coulomb gap on the hopping process is evident), then the unperturbed density of states g_0 and the size of the energy gap Δ may be calculated. These are given by the expressions (Efros and Shklovskii 1975)

$$g_0 = T_c/T_0^2 a_0^3 \text{ K}^{-1} \text{ m}^{-3} = (T_c/T_0^2 a_0^3)\{1.602 \times 10^{-19} \times 10^{-6}/k_B\} \text{ eV}^{-1} \text{ cm}^{-3} \tag{4}$$

and

$$\Delta = (T_0 a_0)^{3/2} g_0^{1/2} \{k_B \times 10^2/1.602 \times 10^{-19}\}^{3/2} \text{ eV} \tag{5}$$

where $a_0 = \alpha^{-1}$ as before. The factors in braces {} are included to convert the units of g_0 and Δ from SI to eV^{-1} cm^{-3} and eV respectively. The calculated values of α, g_0 and Δ for the insulating samples are all given in table 3.

The results for the tunnelling exponent α show reasonable agreement with the results of Knotek *et al* (1973), who determined that α^{-1} lay between 8 Å and 14 Å in pure a-Ge. As can be seen from table 3, α decreases as the Fe concentration is increased in the present samples. This is consistent with the delocalization of the states as the metal–insulator transition is approached from the insulating side. The value of α for sample 8 (15.7 at.% Fe) is seen to lie off the trend of increasing α with decreasing Fe concentration. This is probably due to the poor determination of T_0 as a result of the very limited temperature range over which the data could be fitted, or the sample may consist of both metallic and insulating regions.

The density of states determined from our measurements is higher than the $\sim 10^{18}$ eV^{-1} cm^{-3} reported for pure a-Ge (Knotek *et al* 1973, Nath *et al* 1975) as would be expected. The present results are however lower than the value of $\sim 10^{21}$ eV^{-1} cm^{-3} calculated by Nath *et al* (1975) from their resistivity measurements of Fe_xGe_{1-x} samples with between 2 and 30 at.% Fe. This is not surprising as the data in the latter case were analysed using $\exp(T_0/T)^{1/4}$, against the $\exp(T_0/T)^{1/2}$ used here. Efros and Shklovskii (1975) also

determined the size of the Coulomb gap in pure a-Ge from the measurements of Knotek *et al* (1973), and found $\Delta = 1 \times 10^{-3}$ eV. Therefore, our measurements indicate an increase in the size of the gap by an order of magnitude with the addition of 5 at.% Fe to the Ge, but as the concentration of Fe is further increased, the size of the gap decreases. This behaviour of the energy gap Δ and the behaviour of the density of states g_0 with increasing Fe concentration are shown in figure 6. Previous workers on the a-Fe_xGe_{1-x} system have reported $\rho \propto \exp(T_0/T)^{1/4}$ and hence according to theory there is no energy gap, and so their published results cannot be compared with the present measurements. However, the present extracted values of the energy gap with decreasing Fe concentration in a-Fe_xGe_{1-x} are consistent with the results of Aleshin *et al* (1988) for Cr_xGe_{1-x} films above 1 K.

The divergence of the density of states g_0 and the decrease of the size of the energy gap Δ with increasing concentration, shown in figure 6, indicate that the metal–insulator transition does indeed occur at about 16 at.% Fe. This concentration is also confirmed in the next section which deals with the samples on the metallic side of the transition. Möbius *et al* (1985), from their measurements on a-Cr_xSi_{1-x} have considered the scaling behaviour of $T_0 \simeq (1 - N/N_c)^{\nu}$. Those authors found $\nu \simeq 4$, and extrapolated to $T_0 = 0$ to obtain N_c (Eytan *et al* (1992), from their measurements on granular Al/Ge, found that T_0 goes to zero at the critical metal–insulator volume fraction). In the present measurements on the a-Fe_xGe_{1-x} system, $\nu = 3$ behaviour is observed, but the extrapolated value of N_c at $T_0 = 0$ is 17.6 at.% Fe, in contrast to the value of $N_c = 16$ at.% Fe deduced from other considerations.

4.2. Metallic samples (> 16 at.% Fe)

As electron–electron interactions (Altshuler and Aronov 1979, Altshuler *et al* 1980, Fukuyama 1980, 1981) and weak localization (Gorkov *et al* 1979, Bergmann 1983a, b, 1984, Kawabata 1980a, b) are important in the interpretation of the resistivity in these samples, a brief summary of the relevant equations is given below.

The change in the conductivity due to *electron–electron interaction* effects in 3D films has been expressed by Lee and Ramakrishnan (1985) in the form

$$\Delta\sigma = -\Delta\rho/\rho^2 = (e^2/4\pi^2\hbar)(1.3/\sqrt{2})(\tfrac{4}{3} - \tfrac{3}{2}\tilde{F}_\sigma)\sqrt{T/D} \tag{6}$$

where $\tilde{F}_\sigma$ is the screening parameter for the Coulomb interaction and depends on the Fermi wave vector k_F and D is the diffusion constant. The sign of this correction to the conductivity may be either negative or positive, depending on the size of $\tilde{F}_\sigma$, which is however usually less than $\frac{8}{9}$. Irrespective of the size of $\tilde{F}_\sigma$, the magnetoresistance arising from electron–electron interactions has been shown to be positive, proportional to B^2 for high T or low B, and proportional to $\sqrt{B}$ for low T or high B (Altshuler *et al* 1981, Lee and Ramakrishnan 1982). The observation of such a positive magnetoresistance can arguably be taken as a necessary condition before the dominance of electron–electron interactions may be inferred.

In three dimensions, the conductivity due to *weak localization*, with no spin–orbit scattering, is (Lee and Ramakrishnan 1985)

$$\sigma_{3D}(T) = \sigma_B + [(e^2/\hbar\pi^3)/a]T^{p/2} \tag{7}$$

where σ_B is the Boltzmann conductivity, a is a microscopic scale length of order k_F^{-1}, and p is an index that depends on the scattering mechanism. Clearly then, the temperature dependence of the conductivity depends on the inelastic scattering mechanism through the

index p: $p = 1$ for scattering by phonons (or magnons) at $T > T_D$ (or T_N); $p = 2$ for inelastic electron–electron scattering; $p = 4$ for scattering by phonons or magnons at $T < T_D$ or T_N. The magnetoresistance due to weak localization is negative, proportional to B^2 for high T or low B, and proportional to $\sqrt{B}$ for low T or high B (Kawabata 1980a, b).

Previous work on the Fe_xGe_{1-x} amorphous alloy system between 0 and 30 at.% Fe by Massenet *et al* (1974), in the temperature range 20–300 K, has concluded that $\exp(T_0/T)^{1/4}$ variable-range hopping is observed up to about 25 at.% Fe, above which the conduction was metallic. However, Mott and Kaveh (1985) have subsequently interpreted the samples of Massenet *et al* (1974) with more than 10 at.% Fe as being metallic. Measurements of the resistivity of the a-Fe_xGe_{1-x} system have also been reported by Cros (1980, 1981) for samples with more than 30 at.% Fe. These samples were metallic and at 4.2 K showed no ferromagnetic ordering below 43 at.% Fe, and no spin-glass ordering below 30 at.% Fe. As far as the authors are aware, no magnetoresistance has previously been reported in either insulating or metallic samples with less than 30 at.% Fe. Negative magnetoresistance has however been observed in this system for > 30 at.% Fe (Cros 1980, 1981) in the temperature range 1.3–20 K. Resistivity work on insulating and metallic a-Cr_xGe_{1-x}, which is a very similar system, has been reported by Möbius *et al* (1985) and Elefant *et al* (1991).

The negative temperature coefficient of resistance above about 50 K and the levelling off of the resistivity below this temperature is widely known for amorphous and indeed all high-resistivity metallic systems (Mooij 1973, Tsuei 1986). It is generally associated with the electronic mean free path becoming comparable to the Fermi wavelength (Kaveh and Mott 1982, McLachlan 1982, Tsuei 1986). The sharp increase in the resistivity below $\sim$ 10 K shown in figure 2 and observed in all the metallic samples has not to the authors' knowledge been reported in the Fe_xGe_{1-x} system before, probably as previous experiments did not extend to low enough temperatures. It must be noted however that an increase in the resistivity proportional to $-\sqrt{T}$ has been widely reported for amorphous and highly disordered metals below about 10 K, and Cochrane and Strom-Olsen (1984) list many examples of such behaviour in amorphous alloys in both magnetic and non-magnetic systems. This increase in the resistivity at low temperatures (typically below 10 K) is normally taken to be a manifestation of weak localization and/or electron–electron interactions.

Two models to explain the anomalous behaviour of the resistivity below about 50 K as shown in figure 2 currently appear in the literature:

(1) Elefant *et al* (1991), who base their model solely on their resistivity results, have interpreted the dip in the resistivity as T is decreased below about 50 K as due to electron–electron interactions with $\tilde{F}_\sigma > \frac{8}{9}$ in (6), and suggest that the increase in the resistivity observed below about 10 K is associated with the magnetic properties of the chromium atoms in their samples.

(2) Mott (1990b) and Mott and Davis (1991) support the interpretation of the dip in the resistivity below about 50 K as due to electron–electron interactions with $\tilde{F}_\sigma > \frac{8}{9}$, but they postulate that the increase in resistivity observed below about 10 K is due to weak localization. These authors suggest that if an amorphous alloy contains an atom with a magnetic moment, weak localization will be damped out by magnons above about 4 K, but will manifest itself below about 4 K with a $\rho \propto -\sqrt{T}$ dependence. This temperature dependence of the resistivity is determined from (7), with the inelastic scattering time $\tau_i \propto T^{-1}$ due to scattering from magnons above the Néel temperature T_N (Mott 1990a), and hence $L_i = (D\tau_i)^{1/2}$ is proportional to $T^{-1/2}$. Note that this model requires that T_N be about 100 mK or lower in the present samples, and below about 500 mK in metallic a-Cr_xGe_{1-x}.

The results presented in the current study will be examined in terms of these models. The behaviour of both the temperature coefficient of resistance and the magnetoresistance will be used to indicate which of the two mechanisms is dominant in which temperature region.

Sample 1 (28.0 at.% Fe) shows qualitative agreement with the results of measurements on samples with > 30 at.% Fe reported by Cros (1980), where the two temperature ranges overlap. The magnetoresistance in this particular sample is negative for all temperatures below 5 K, where it appears to follow a B^2 behaviour for low fields but starts saturating above about 1 T. This magnetoresistance behaviour is also very similar to that observed by Cros (1980) for samples with > 30 at.% Fe; he interpreted his data in terms of magnetic scattering as described by the theory of Béal-Monod and Weiner (1968).

The resistivity of samples 2–7 (23–16 at.% Fe) behaves in a similar manner to that of sample 1 (28.0 at.% Fe), except that the plateau region below 50 K has changed into a distinct maximum followed by a decrease in the resistivity in some samples (numbers 2, 3, and 4), before the sharp increase in resistivity below 10 K (see figure 2). The increase in the resistivity of samples 2, 3, and 4 (23.2 at.%, 20.5 at.%, and 20.1 at.% Fe) below about 10 K shows a $\rho \propto -\sqrt{T}$ dependence (figure 3). If the decrease in resistivity below 50 K is taken to be due to electron–electron interactions with $\tilde{F}_\sigma > \frac{8}{9}$, the same mechanism cannot be responsible for the observed increase in ρ below 10 K. This is confirmed by the observation of positive magnetoresistance in the region of 2–4 K, followed by a changeover to negative magnetoresistance at lower temperatures. Therefore weak localization with no spin–orbit coupling, which is characterized by a negative magnetoresistance, may well be the dominant mechanism responsible for the $\rho \propto -\sqrt{T}$ increase in the resistivity observed below 10 K, as postulated by the second model.

At 4 K the magnetoresistance in metallic samples 2–7 (23.2–16.5 at.% Fe) is positive, initially proportional to B^2 for very small B, but changing to a $B^{3/2}$ dependence for $B \gtrsim 1$ T. The observed $B^{3/2}$ dependence could be an intermediate between the low-field B^2 dependence and a $B^{1/2}$ dependence at higher fields, as expected from the theory for electron–electron interactions. However, measurements at higher fields are needed to confirm this conjecture. The observed magnetoresistance behaviour in the present measurements is therefore not fully consistent with the behaviour due to electron–electron interactions. On cooling these samples below 4 K, the magnitude of the positive magnetoresistance at 3.86 T goes through a maximum and then decreases, becoming negative at some concentration-dependent lower temperature. Below the changeover temperature from positive to negative magnetoresistance, the field dependence of the magnetoresistance is also different, the magnitude increasing (in a negative sense) for fields less than about 2 T, and then decreasing slightly for larger fields (figure 4(*b*)). However, the observed decrease in the resistivity in the range 50–10 K cannot at this stage be definitely ascribed to electron–electron interactions, because of the discrepancy between the form of the magnetoresistance expected from the theory for electron–electron interactions, and the magnetoresistance observed over the measured range of B.

In order to try to correlate the negative magnetoresistance and the $-\sqrt{T}$ dependence of the resistivity in samples 2–7, the changeover temperature from positive to negative magnetoresistance in fields of 0.95 T and 3.86 T, together with the highest temperature at which the $-\sqrt{T}$ dependence in the resistivity is observed, are plotted as functions of the Fe concentration in figure 7. From this figure it is clear that some correlation exists between the $-\sqrt{T}$ dependence in the resistivity and the negative magnetoresistance, which further supports the second model. Note in figure 7 that in the 15.7 at.% Fe sample (sample 8) the changeover temperature from positive to negative magnetoresistance is off the general trend,

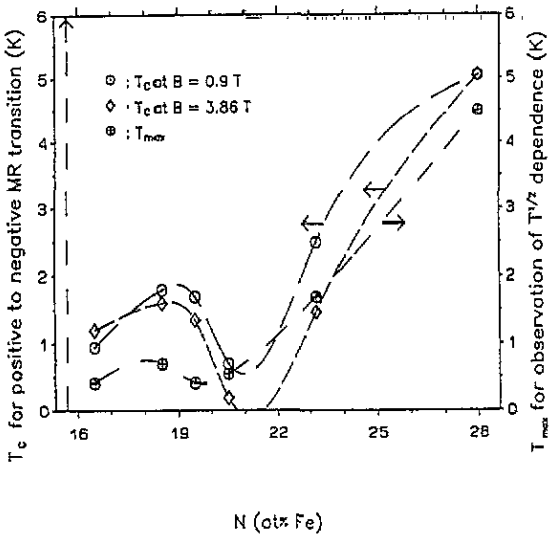

Figure 7. The crossover temperature T_c from positive to negative magnetoresistance in 0.95 T and 3.86 T against the concentration of Fe on the metallic side of the transition (sample 4: 20.1 at.% Fe not included). Note that sample 8 (15.7 at.% Fe) has $T_c > 6$ K, and so there is a definite discontinuity in the magnetoresistance behaviour between 15.7 at.% and 16.5 at.% Fe. Also plotted is the highest temperature T_{max} at which a clear $\sqrt{T}$ dependence is observed in ρ. Note the remarkable similarity between T_c and T_{max} as a function of Fe concentration. The lines are drawn to guide the eye.

lying above 6 K, showing a fundamental difference between the 16.5 at.% and 15.7 at.% Fe samples.

Unfortunately, Elefant *et al* (1991), in presenting their results of the resistivity in the a-Cr_xGe_{1-x} ($0.14 \leqslant x \leqslant 0.20$) system, neither give an exact temperature dependence of the resistivity below about 5 K nor do they present any magnetoresistance results. Similar behaviour to that observed here in the magnetoresistance (positive above about 1.5 K, negative below) near the metal–insulator transition has been reported for a-Cr_xGe_{1-x} films ($0.08 \leqslant x \leqslant 0.11$) in the temperature range 4–0.47 K by Aleshin *et al* (1988). However none of their results show the $\rho \propto -\sqrt{T}$ increase in the resistivity shown by all metallic Fe_xGe_{1-x} samples at sufficiently low temperatures. Aleshin *et al* (1988) interpreted the negative magnetoresistance observed below about 1.5 K as evidence for a spin-glass-type magnetic ordering in a-Cr_xGe_{1-x} with $x < 0.11$. The limited data presented by these authors and the general uncertainty in the field make detailed comparison with the present results impossible.

The sample with 28 at.% Fe (sample 1) has previously been discussed separately to compare it with similar samples of Cros (1980, 1981) and because it shows negative magnetoresistance at all temperatures below 5 K. Considering figure 7 however, it is clear that this sample is consistent with the other metallic samples, with its magnetoresistance behaviour being dominated by weak localization below 5 K. Very similar ρ and negative magnetoresistance behaviour has been observed by Cros (1980, 1981) in samples with more than 30 at.% Fe, but no observable magnetoresistance was found in the sample with 30 at.% Fe. Cros attributed the negative magnetoresistance behaviour observed in samples with more than 30 at.% Fe to the magnetism of the samples. This hypothesis agrees with the first model.

The dip in the resistivity as the temperature is decreased below about 50 K, which has only been observed in amorphous alloys containing magnetic atoms (Cr and Fe), has been attributed to electron–electron interactions with $\tilde{F}_\sigma > \frac{8}{9}$ in the previous papers. Such an abnormally large value for $\tilde{F}_\sigma$ may therefore be magnetic in origin. In the present work it is found that the temperature dependence of the resistivity is consistent with this interpretation, although the observed magnetoresistance may not be. A similar decrease in the resistivity, with the maximum lying between 15 and 45 K, has been reported in the a-Fe_xZr_{1-x} system close to and on either side of the paramagnetic to ferromagnetic transition (Strom-Olsen *et al* 1985). These authors attribute this behaviour to the influence of spin fluctuations. It has also been reported (Trudeau and Cochrane 1988) that the influence of spin fluctuations may be incorporated in the expression for electron–electron interactions (6) through an enhanced value of $\tilde{F}_\sigma$. This mechanism may therefore be responsible for the observed dip in the resistivity in the Fe_xGe_{1-x} system as well. However it should be noted that for the Fe_xGe_{1-x} system it has been widely reported (see, for example, Massenet and Daver 1978, Massenet *et al* 1979, Buschow and van Engen 1981, Morrison *et al* 1985) that the magnetic moment of the Fe atoms in Fe_xGe_{1-x} with less than 25 at.% Fe is removed through hybridization of the Fe d band with the orbitals of the Ge atoms. It is also interesting to note from figure 7 that the $\rho \propto -\sqrt{T}$ dependence and the negative magnetoresistance are observed at higher temperatures in samples with higher concentrations of Fe. If the $\rho \propto -\sqrt{T}$ dependence and the negative magnetoresistance are interpreted as being due to weak localization (following the second model), this indicates that the damping out of weak localization by magnons becomes less effective with increasing Fe concentration, which is counterintuitive.

A different interpretation of the resistivity behaviour observed below 50 K in the metallic Fe_xGe_{1-x} samples presented here may be considered. The observed decrease in the resistivity as the temperature decreases below 50 K could be interpreted as due to weak anti-localization, with a positive magnetoresistance. The observed $\rho \propto -\sqrt{T}$ increase below about 5 K could then be interpreted as being due to electron–electron interactions beginning to dominate. This interpretation however requires positive magnetoresistance at the lowest temperatures, due to the electron–electron interactions, which is contrary to the observed negative magnetoresistance. This interpretation is thus not consistent with the resistivity and magnetoresistance behaviour observed in the metallic Fe_xGe_{1-x} samples below about 50 K.

In conclusion, the present authors find that well on the high-temperature side of the minimum in the resistivity, the change in the resistivity appears to be dominated by electron–electron interactions, which give a positive temperature coefficient of resistance. However, over the measured range of B we have been unable to establish whether the magnetoresistance is due to electron–electron interactions or not. At the lowest temperatures, we believe that a different mechanism, namely weak localization, dominates, which gives a negative temperature coefficient of resistance and negative magnetoresistance. However, the temperature at which the change in sign occurs for the temperature coefficient of resistance and the magnetoresistance is not the same. The authors do not believe this to be a requirement of the theories. The positive magnetoresistance observed in the metallic samples between about 2.5 K and 4 K may thus be associated with the positive temperature coefficient of resistance observed between about 10 K and 50 K, but the field dependence in the measured field range is not consistent with the interpretation of either the first or the second model. The resistivity and magnetoresistance behaviour observed below about 2.5 K (in the negative magnetoresistance region) and the resistivity observed between about 10 K and 50 K in the metallic samples in the present study support the interpretation proposed

in the second model. This model however requires that the Fe moment be only weakened and not removed by any hybridization that may occur.

4.3. The metal–insulator transition

The resistivity in the temperature range where the $-\sqrt{T}$ dependence is observed in these metallic samples has been fitted using the expression

$$\sigma(T) = \sigma(0) + CT^{1/2} \tag{8}$$

using MINUIT, with the fitting parameters $\sigma(0)$ and C. The values obtained for these parameters are shown in table 4. From this table, it can be seen that $\sigma(0)$ varies from 500 Ω^{-1} cm^{-1} for the sample with 28 at.% Fe to 9 Ω^{-1} cm^{-1} for the sample with 16.5 at.% Fe. The disappearance of $\sigma(0)$ as the metal–insulator transition is approached from the metallic side is widely used as a criterion for the transition, and the current data indicate that the metal–insulator transition occurs between the 15.7 at.% Fe sample which appears to show hopping behaviour below 2 K, and the 16.5 at.% Fe sample. In this case, because $[(n/n_c) - 1] > 0.05$, $\sigma(0)$ is not expected to follow scaling behaviour of the form $\sigma(0) = \sigma_c[(n/n_c) - 1]^{\nu}$ (Rosenbaum *et al* 1983).

Table 4. Values of the parameters $\sigma(0)$ and C determined by fitting the σ versus T data to the expression $\sigma(T) = \sigma(0) + CT^{1/2}$.

Sample	$\sigma(0)$ (Ω^{-1} cm^{-1})	C (Ω^{-1} cm^{-1} K$^{-1/2}$)	T_{max} (K)
1 (28.0 at.% Fe)	500(20)	25(2)	4.5
2 (23.2 at.% Fe)	360(30)	26(5)	1.7
3 (20.5 at.% Fe)	300(20)	27(5)	0.55
5 (19.5 at.% Fe)	31(2)	34(1)	0.42
6 (18.5 at.% Fe)	47(4)	23(1)	0.70
7 (16.5 at.% Fe)	9(1)	17(1)	0.42

As a first approximation, assuming between 0.4 and 1 electron per Fe atom (Massenet and Daver 1977) and no electrons per Ge atom, and calculating the packing density of a-$Fe_{0.157}Ge_{0.843}$ with respect to crystalline Ge as 93.5% (using the radial distribution function results of Temkin *et al* (1974) for a-Ge, and of Uemura *et al* (1977) for a-Fe_xGe_{1-x}), the critical carrier concentration n_c can be calcualted to lie between 2.9×10^{21} cm^{-3} and 7.3×10^{21} cm^{-3}. The effective Bohr radius (a_H^*) of the electrons in the a-Fe_xGe_{1-x} system near the metal–insulator transition can then be calculated using the Mott criterion (Mott 1974, Mott and Davis 1979)

$$n_c^{1/3} a_H^* \simeq 0.25. \tag{9}$$

Inserting the values of n_c calculated above yields a value of a_H^* between 1.75 Å and 1.29 Å. These values are an order of magnitude smaller than the $a_0 = \alpha^{-1}$ ($a_0 = 40$ Å for 15.7 at.% Fe) calculated from the theory of Efros and Shklovskii and a factor of 2–4 smaller than the estimated mean Fe–Fe separation for 10 at.% Fe in Ge of between 5 Å and 8 Å. This discrepancy has also been pointed out by Abkemeier *et al* (1992) from their results on the a-Ni_xSi_{1-x} system. Using the radial distribution function results of Uemura *et al* (1977), the mean radius of the Wigner–Seitz cell in a-$Fe_{0.1}Ge_{0.9}$ is calculated to be 1.25 Å. Therefore, (9) applied to our result indicates that the conduction electrons are localized approximately within the Wigner–Seitz cell of the Fe atoms in the amorphous lattice.

Acknowledgments

The authors wish to thank Professor Ralph Rosenbaum for enlightening discussions and his critical reading of an early version of the manuscript.

References

Abkemeier K M, Adkins C J, Asal R and Davis E A, 1992 *J. Phys.: Condens. Matter* **4** 46
Adkins C J 1989 *J. Phys.: Condens. Matter* **1** 1253
Aleshin A N, Ionov A N, Parfen'ev R V, Shlimak I S, Heinrich A, Schumann J and Elefant D 1988 *Fiz. Tverd. Tela* **30** 696 (Engl. transl. 1988 *Sov. Phys.–Solid State* **30** 398)
Altshuler B L and Aronov A G 1979 *Solid State Commun.* **30** 115
Altshuler B L, Aronov A G, Larkin A I and Kmelnitskii D E 1981 *Sov. Phys.–JETP* **54** 411
Altshuler B L, Aronov A G and Lee P A 1980 *Phys. Rev. Lett.* **44** 1288
Béal-Monod M-T and Weiner R A 1968 *Phys. Rev.* **170** 552
Bergmann G 1983a *Phys. Rev.* B **28** 515
—— 1983b *Phys. Rev.* B **28** 2914
—— 1984 *Phys. Rep.* **107** 1
Buschow K H J and van Engen P G 1981 *J. Appl. Phys.* **52** 3557
Chopra K L and Nath P 1976 *Phys. Status Solidi* a **33** 333
Cochrane R W and Strom-Olsen J O 1984 *Phys. Rev.* B **29** 1088
Cros Y 1980 *PhD Thesis* Universite Scientifique & Medicale de Grenoble
—— 1981 *J. Appl. Phys.* **52** 2196
Daver H, Massenet O and Chakraverty B K 1974 *Proc. 5th Int. Conf. on Amorphous and Liquid Semiconductors (Garmisch-Partenkirchen, 1973)* (London: Taylor and Francis) p 1053
Efros A L and Shklovskii B I 1975 *J. Phys. C: Solid State Phys.* **8** L49
Elefant D, Gladun C, Heinrich A, Schumann J and Vinzelberg H 1991 *Phil. Mag.* B **64** 49
Eytan G, Zaken E, Rosenbaum R, McLachlan D S and Albers A 1992 private communication
Fukuyama H 1980 *J. Phys. Soc. Japan* **48** 2169
—— 1981 *J. Phys. Soc. Japan* **50** 3407
Gorkov L P, Larkin A I and Khmelnitzkii D E 1979 *JETP Lett.* **30** 228
James F and Roos M 1975 *Comput. Phys. Commun.* **10** 343
Kaveh M and Mott N F 1982 *J. Phys. C: Solid State Phys.* **15** L707
Kawabata A 1980a *Solid State Commun.* **34** 431
—— 1980b *J. Phys. Soc. Japan* **49** 628
Knotek M L, Pollak M, Donovan T M and Kurtzman H 1973 *Phys. Rev. Lett.* **30** 853
Lee P A and Ramakrishnan T V 1982 *Phys. Rev.* B **26** 4009
—— 1985 *Rev. Mod. Phys.* **57** 287
Massenet O and Daver H 1977 *Solid State Commun.* **21** 37
—— 1978 *Solid State Commun.* **25** 917
Massenet O, Daver H and Geneste J 1974 *J. Physique Coll.* **35** C4-279
Massenet O, Daver H, Nguyen V D and Rebouillat J P 1979 *J. Phys. F: Met. Phys.* **9** 1687
McLachlan D S 1982 *Solid State Commun.* **42** 521
Möbius A, Vinzelberg H, Gladun C, Heinrich A, Elefant D, Schumann J and Zies G 1985 *J. Phys. C: Solid State Phys.* **18** 3337
Mooij J H 1973 *Phys. Status Solidi* a **17** 521
Morrison T I, Brodsky M B, Zaluzec N J and Sill L R 1985 *Phys. Rev.* B **32** 3107
Mott N F 1968 *J. Non-Cryst. Solids* **1** 1
—— 1974 *Metal–Insulator Transitions* (London: Taylor and Francis)
—— 1990a *Metal–Insulator Transitions* 2nd edn (London: Taylor and Francis)
—— 1990b *Localisation 1990: Proc. Int. Conf. on Localisation (Inst. Phys. Conf. Ser. 108)* ed K A Benedict and J T Chalker (Bristol: Institute of Physics) p 1
Mott N F and Davis E A 1979 *Electronic Processes in Non-Crystalline Materials* (Oxford: Oxford University Press)
—— 1991 private communication
Mott N F and Kaveh M 1985 *Adv. Phys.* **34** 329

Nath P, Barthwal S K and Chopra K L 1975 *Solid State Commun.* **16** 301
Phillips J C 1968 *Phys. Rev. Lett.* **20** 550
Pollak M, Knotek M L, Kurtzman H and Glick H 1973 *Phys. Rev. Lett.* **30** 856
Rosenbaum T F, Milligan R F, Paalanen M A, Thomas G A, Bhatt R N and Lin W 1983 *Phys. Rev.* B **27** 7509
Shklovskii B I and Efros A L 1984 *Electronic Properties of Doped Semiconductors* (Berlin: Springer)
Strom-Olsen J O, Altounian Z, Cochrane R W and Kaiser A B 1985 *Phys. Rev.* B **31** 6116
Temkin R J, Connell G A N and Paul W 1974 *Amorphous and Liquid Semiconductors: Proc. 5th Int. Conf. on Amorphous and Liquid Semiconductors (Garmisch-Partenkirchen, 1973)* (London: Taylor and Francis) p 533
Trudeau M L and Cochrane R W 1988 *Phys. Rev.* B **38** 5353
Tsuei C C 1986 *Phys. Rev. Lett.* **57** 1943
Uemura O, Suzuki Y and Satow T 1977 *Phys. Status Solidi* a **41** 417
Watanabe I, Kawauchi M and Shimizu T 1979 *Japan. J. Appl. Phys.* **18** 453
White H and McLachlan D S 1986 *J. Phys. C: Solid State Phys.* **19** 5415